

First VLBI mapping of a rare SiO isotopic substitution

R. Soria-Ruiz¹, F. Colomer², J. Alcolea¹, V. Bujarrabal², J.-F. Desmurs¹, and K.B. Marvel³

¹ Observatorio Astronómico Nacional, c/Alfonso XII 3, 28014 Madrid, Spain

² Observatorio Astronómico Nacional, Apartado 112, 28803 Alcalá de Henares, Spain

³ American Astronomical Society, 2000 Florida Avenue NW Suite, Washington, DC-20009-1231, USA

Abstract. We report the first VLBI map of the 7 mm $v=0 J=1-0$ maser line of the ^{29}SiO isotopic substitution in the long period variable star IRC +10011. We have found that this maser emission is composed of multiple features distributed in an incomplete ring, suggesting that this maser is also amplified tangentially as already proposed in other SiO circumstellar masers. We present also the results for some ^{28}SiO 7 mm and 3 mm maser lines. We confirm in this epoch that the 86 GHz maser $v=1 J=2-1$ in IRC +10011 is formed in an outer region of the circumstellar envelope compared to the other SiO masers studied. The ^{29}SiO maser region appears to be located in a layer in between the $^{28}\text{SiO} v=1 J=1-0$ and $^{28}\text{SiO} v=1 J=2-1$ lines. Finally, we discuss the possible implications of the observational results in the SiO maser pumping theory.

1. Introduction

SiO maser emission is detected in the innermost shells of the circumstellar envelopes around Long Period Variable (LPV) stars. Three different isotopic substitutions of the SiO molecule are known to present maser emission in these objects: ^{28}SiO , ^{29}SiO and ^{30}SiO . The study of this type of emission provides information about the physical processes that occur near the central source.

Very long baseline interferometric (VLBI) observations have also contributed to a better understanding of the SiO maser phenomenon itself, although only the strong 7 mm and recently the 3 mm rotational transitions of ^{28}SiO , which is the most abundant isotopic substitution, have been mapped in these LPVs (see for example Doeleman et al. 1998 and Desmurs et al. 2000). In fact, prior to this work, no VLBI detection of SiO maser lines other than those of the main isotope ^{28}SiO have been reported.

The first single-dish detection of the $^{29}\text{SiO} v=0 J=1-0$ line in IRC +10011 was performed by Cho et al. (1986). Subsequent studies of this circumstellar maser transition revealed that it has some properties usually associated to the ^{28}SiO maser lines, such as its time variability or the correlation with the $8\mu\text{m}$ stellar radiation (Alcolea & Bujarrabal 1992).

In the following sections we present the first map of the $^{29}\text{SiO} v=0 J=1-0$ maser line in an evolved star, IRC +10011, using very long baseline interferometry. We compare the results obtained for this transition with those of the ^{28}SiO lines, and we also discuss how our observational results may affect the ^{29}SiO circumstellar maser theory.

2. Observations and data analysis

The observations of the SiO maser transitions in IRC +10011 were performed on 2002 December 7 using the NRAO¹ Very

Long Baseline Array (VLBA). We observed the $^{29}\text{SiO} v=0 J=1-0$, $^{28}\text{SiO} v=1 J=2-1$, $^{28}\text{SiO} v=1 J=1-0$ and the $^{28}\text{SiO} v=2 J=1-0$ (whose rest frequencies are 42879.916, 86243.442, 43122.080 and 42820.587 MHz respectively).

These observations correspond to the second epoch of a VLBA multi-epoch/transitional study of some SiO maser lines in a sample of AGB stars. All the transitions were detected and mapped. We note that for the first time, we have been able to map the ^{29}SiO emission in a circumstellar envelope.

The data were correlated at NRAO facilities in Socorro (New Mexico). The 43 GHz transitions were recorded simultaneously and separated a few hours to the 86 GHz data. The spectral resolutions achieved were 0.22 km s^{-1} and 0.11 km s^{-1} using a 8 MHz and 16 MHz bandwidths. The calibration was done using the Astronomical Image Processing System (AIPS) package, following the standard procedures for spectral line VLBI observations.

3. Results

We present in Fig. 1 the total power and the recovered maser intensity, after full calibration and imaging, of the different observed transitions. The single-dish spectra are composed of multiple peaks with velocities near the systemic velocity of the source ($V_{LSR} = 9.2\text{ km s}^{-1}$, from Cernicharo et al. 1997). The line profiles of the $v=1$ and $v=2$ $J=1-0$ masers are similar although they differ from the $v=1 J=2-1$ and $^{29}\text{SiO} v=0 J=1-0$ ones.

The integrated intensity maps are shown in Figs. 2 and 3. The $^{29}\text{SiO} v=0 J=1-0$ and $^{28}\text{SiO} v=1 J=2-1$ maser maps are composed of a few spots forming an incomplete ring. In contrast, the ring-like geometry is clear for the $v=1$ and $v=2 J=1-0$ lines. The map of the ^{29}SiO transition (left panel of Fig. 2) is composed of 7 maser spots with velocities ranging from 5.7 to 11.3 km s^{-1} . The brightest feature has an intensity of $\sim 1.76\text{ Jy beam}^{-1} \cdot \text{km s}^{-1}$. The ^{29}SiO emission is the weakest among the four lines observed. The emission forms a ring, though incomplete, with a mean radius of $\sim 13.5\text{ mas}$, therefore this maser

¹ The National Radio Astronomy Observatory is a facility of the National Science Foundation operated under cooperative agreement by Associated Universities, Inc.

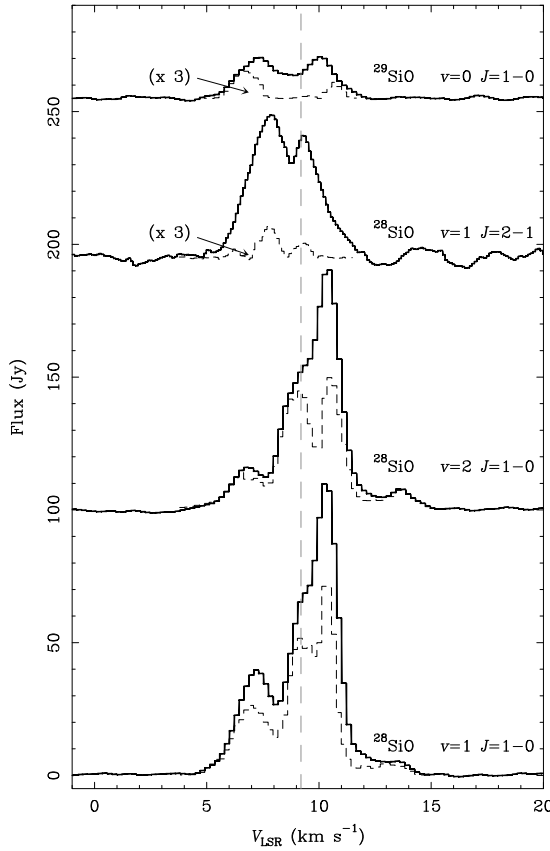


Fig. 1. The total power (continuous lines) and recovered flux (dashed lines) spectra in IRC +10011. The dashed grey line indicates the systemic velocity of the source.

radiation is probably amplified tangentially, as other well studied maser transitions.

From the comparison of rotational transitions within the same vibrational state, the ^{28}SiO $v=1$ $J=1-0$ and $J=2-1$, we obtained that the latter line is produced in a layer further away than the $J=1-0$ one. Furthermore, the ^{29}SiO $v=0$ $J=1-0$ maser region appears to be located in a layer in between these two transitions. In this case, the spatial distributions of the $v=1$ regions clearly differ (right and left panels of Figs. 2 and 3). This result is compatible with that obtained in previous observations of IRC +10011 (see Fig. 4).

The $v=1$ and $v=2$ $J=1-0$ ^{28}SiO lines (Fig. 3) present ring structures composed of multiple spots with similar distributions. In IRC +10011, Desmurs et al. (2000) and Soria-Ruiz et al. (2004) found a systematic shift between these two lines of about 1–3 mas, being the $v=2$ always located in an inner region of the envelope. We confirm this result since our $v=1$ and $v=2$ maps are displaced ~ 1 mas (see Fig. 3). We note that similar angular shifts have also been measured in other Mira variable stars (Cotton et al. 2004).

Furthermore, although the observational results are consistent with those obtained in the first epoch, there are some small differences when comparing the maps. For example, the 86 GHz ^{28}SiO $v=1$ $J=2-1$ emission is distributed in different regions of the circumstellar envelope (see both panels of Fig. 4). However, this is not the case of the 43 GHz masers, the

^{28}SiO $v=1$ $J=1-0$ and ^{28}SiO $v=2$ $J=1-0$, which show in both epochs some maser features in common.

4. Discussion

Some theoretical models have been proposed to explain the ^{29}SiO $v=0$ $J=1-0$ maser amplification in these evolved stars. Robinson & Van Blerkom (1981) and Deguchi & Nguyen-Quang-Rieu (1983) suggested that this ground-state masers were produced if the vibrational transitions present a significantly higher opacity along the radial direction than in the tangential one, predicting a two-peaked line profiles similar to the circumstellar OH lines. However, the model does not reproduce the observations since the line shapes of ^{29}SiO masers are composed of narrow peaks near the stellar velocity (Alcolea & Bujarrabal 1992), and, in addition, our maps indicate a ring-like geometry, very probably due to tangential amplification.

Other physical mechanisms involved in the SiO excitation are the line overlaps between infrared transitions of ^{28}SiO and ^{29}SiO . Those were firstly suggested by Olofsson et al. (1981) to explain the $v=0$ ^{29}SiO maser lines. Subsequent calculations by Cernicharo et al. (1997) indicate that the $v=0$ $J=1-0$ ^{29}SiO line might be effectively pumped by the overlap between the ^{28}SiO $v=2$ $J=4 \rightarrow v=1$ $J=3$ and the ^{29}SiO $v=1$ $J=0 \rightarrow v=0$ $J=0$ ro-vibrational transitions.

The fact that the $v=0$ $J=1-0$ ^{29}SiO maser is confined in a region of the envelope in between the ^{28}SiO $v=1$ $J=1-0$ and $J=2-1$ masing shells, indicates that this maser line requires high excitation temperatures ($T_{ex} \sim 1700$ K). This can be explained if the inversion population of the ground state is mainly produced via de-excitations from the $v > 0$ vibrational levels. In addition, one possible process to pump the ^{29}SiO $v=0$ $J=1-0$ line could be the frequency overlap with different ro-vibrational transitions of abundant molecules, such as ^{28}SiO , H_2O , or others.

However, none of these theories explain how their excitation mechanisms affect the spatial distribution of the different ^{28}SiO and ^{29}SiO maser lines. Therefore, this makes very difficult to compare our observational results with the predictions of the proposed ^{29}SiO pumping models.

This type of observations, where multiple SiO maser transitions are measured, allow us to compare directly regions of the envelope with different physical conditions. Moreover, from these presented VLBA images, we can see that the width of the whole masing shell is considerable (~ 7 – 9 mas) and may not be as thin as that obtained from the observations of a single maser line.

5. Summary and work in progress

We have presented the first image of the ^{29}SiO $v=0$ $J=1-0$ maser line in a late type star, IRC +10011. The distribution of the emission suggests that, as in other well studied circumstellar masers, the amplification is tangential. The maser shell is ring-like, and located in a region in between the ^{28}SiO $v=1$ $J=2-1$ and $v=1$ $J=1-0$ rings.

We confirm that the $v=1$ $J=2-1$ maser (86 GHz) in IRC +10011 is formed further away from the central AGB star,

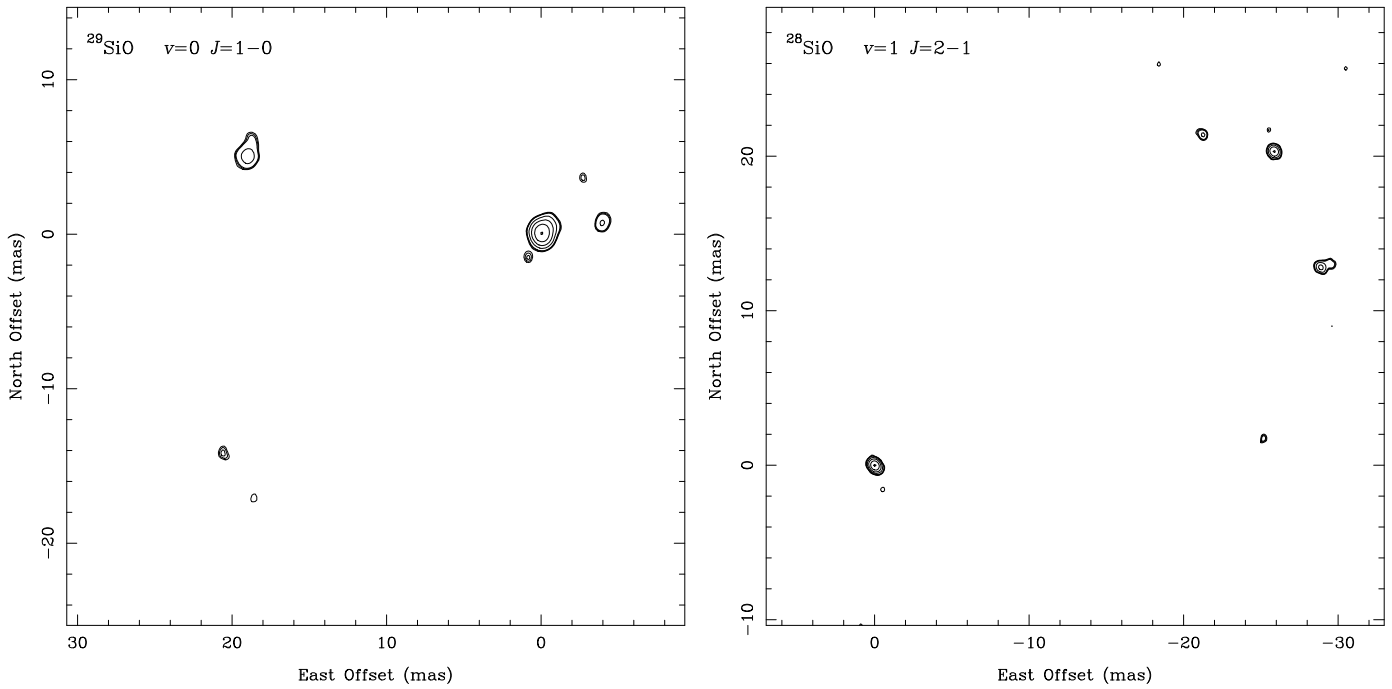


Fig. 2. Integrated intensity maps for the ^{29}SiO $v=0$ $J=1-0$ (left) and ^{28}SiO $v=1$ $J=2-1$ (right) masers in IRC+10011. The peak flux is 1.77 and 2.41 Jy $\text{beam}^{-1} \cdot \text{km s}^{-1}$ respectively. The contour levels are 0.08, 0.10, 0.12, 0.23, 0.46, 0.92 and 1.76 Jy $\text{beam}^{-1} \cdot \text{km s}^{-1}$ for the $J=1-0$ and 0.10, 0.12, 0.14, 0.28, 0.57, 1.14 and 2.28 Jy $\text{beam}^{-1} \cdot \text{km s}^{-1}$ for the $J=2-1$.

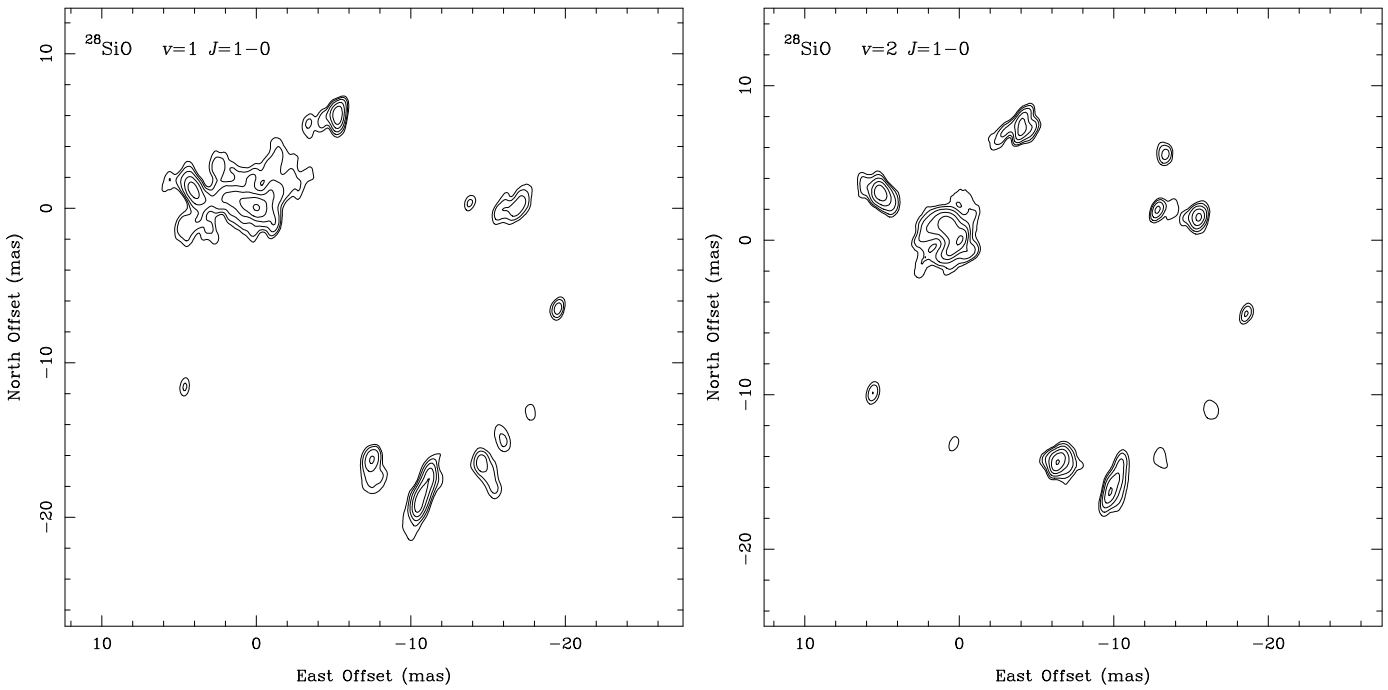


Fig. 3. Integrated intensity maps for the ^{28}SiO $v=1$ (left) and $v=2$ (right) $J=1-0$ rotational transitions in IRC+10011. The peak flux is 9.14 and 9.72 Jy $\text{beam}^{-1} \cdot \text{km s}^{-1}$ respectively. The contour levels in both images are 0.28, 0.57, 1.14, 2.28, 4.16 and 8.34 Jy $\text{beam}^{-1} \cdot \text{km s}^{-1}$.

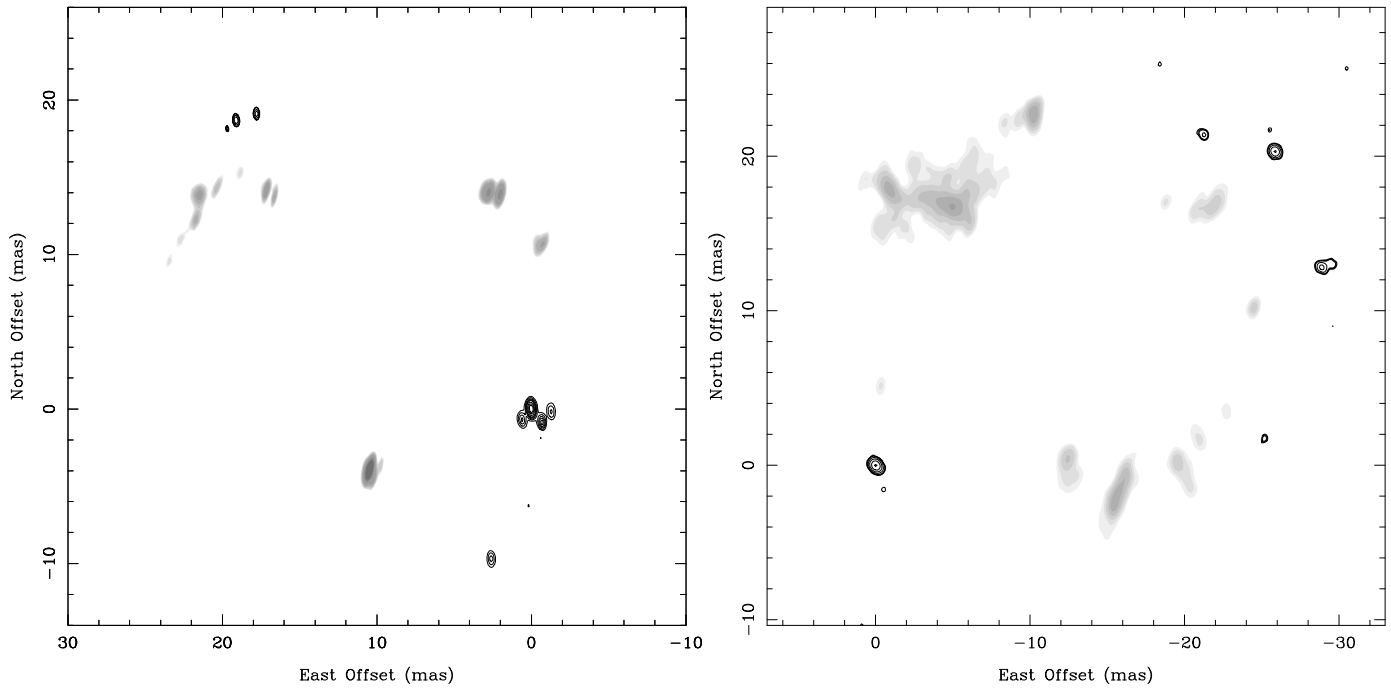


Fig. 4. Comparison of the ^{28}SiO $v=1$ $J=1-0$ (grey) and $J=2-1$ (line contours) rotational transitions in IRC+10011. Left: results from Soria-Ruiz et al. (2004). Right: results of this work.

and that the $v=1$ and $v=2$ $J=1-0$ (43 GHz) maser regions have a similar distribution, though clearly not identical.

At present we are analyzing the same observed SiO masers in other variable stars: R Leo, TX Cam and χ Cyg. We are also introducing the line overlaps in the theoretical pumping calculations of the ^{29}SiO emission to study the possible physical processes involved in this peculiar amplification effect.

Acknowledgements. This work has been financially supported by the Spanish DGI (MCYT) under projects AYA2000-0927 and AYA2003-7584, and by the European Commission's I3 Programme “RADIONET”, under contract No. 505818.

References

Alcolea, J. & Bujarrabal, V. 1992, A&A, 253, 475
 Cernicharo, J., Alcolea, J., Baudry, A., & González-Alfonso, E. 1997, A&A, 319, 607
 Cho, S.-H., Kaifu, N., Ukita, N., Morimoto, M., & Hayashi, M. 1986, Ap&SS, 118, 237
 Cotton, W.D., Mennesson, B., Diamond, P.J., et al. 2004, A&A, 414, 275
 Deguchi, S. & Nguyen-Quang-Rieu 1983, A&A, 117, 314
 Desmurs, J.-F., Bujarrabal, V., Colomer, F., & Alcolea, J. 2000, A&A, 360, 189
 Doeleman, S.S., Lonsdale, C.J., & Greenhill, L.J. 1998, ApJ, 494, 400
 Olofsson, H., Hjalmarsson, A., & Rydbeck, O.E.H. 1981, A&A, 100, L30
 Robinson, S.E. & Van Blerkom, D.J., ApJ, 249, 566
 Soria-Ruiz, R., Alcolea, J., Colomer, F., et al. 2004, A&A, in press